THE JOURNAL OF BIOLOGICAL CHEMISTRY
Vol. 273, No. 33, Issue of August 14, pp. 20972–20981, 1998

Printed in U.S.A.

Characterization of a Rat Na^+-Dicarboxylate Cotransporter*

(Received for publication, April 22, 1998, and in revised form, June 11, 1998)

Xing-Zhen Chen, Chairat Shayakul, Urs V. Berger, Wei Tian, and Matthias A. Hediger‡

From the Renal Division, Brigham and Women's Hospital, Harvard Medical School, Boston, Massachusetts 02115

The metabolism of Krebs cycle intermediates is of fundamental importance for eukaryotic cells. In the kidney, these intermediates are transported actively into epithelial cells. Because citrate is a potent inhibitor for calcium stone formation, excessive uptake results in nephrolithiasis due to hypocitraturia. We report the cloning and characterization of a rat kidney dicarboxylate transporter (SDCT1). *In situ* hybridization revealed that SDCT1 mRNA is localized in S3 segments of kidney proximal tubules and in enterocytes lining the intestinal villi. Signals were also detected in lung bronchioli, the epididymis, and liver. When expressed in *Xenopus* oocytes, SDCT1 mediated electrogenic, sodium-dependent transport of most Krebs cycle intermediates (K_m = 20–60 μM), including citrate, succinate, α-ketoglutarate, and oxaloacetate. Of note, the acidic amino acids L- and D-glutamate and aspartate were also transported, although with lower affinity (K_m = 2–18 mM). Transport of citrate was pH-sensitive. At pH 7.5, the K_m for citrate was high (0.64 mM), whereas at pH 5.5, the K_m was low (57 μM). This is consistent with the concept that the −2 form of citrate is the transported species. In addition, maximal currents at pH 5.5 were 70% higher than those at pH 7.5, and our data show that the −3 form acts as a competitive inhibitor. Simultaneous measurements of substrate-evoked currents and tracer uptakes under voltage-clamp condition, as well as a thermodynamic approach, gave a Na^+ to citrate or a Na^+ to succinate stoichiometry of 3 to 1. SDCT1-mediated currents were inhibited by phloretin. This plant glycoside also inhibited the SDCT1-specific sodium leak in the absence of substrate, indicating that at least one Na^+ binds to the transporter before the substrate. The data presented provide new insights into the biophysical characteristics and physiological implications of a cloned dicarboxylate transporter.

In kidney proximal tubules, reabsorption of Krebs cycle intermediates such as citrate, succinate, α-ketoglutarate, malate, and fumarate has been shown to be accomplished by Na^+-coupled transporters (1–9). Numerous studies have been performed in intact proximal tubules (10), isolated brush border membrane vesicles (BBMV)[1] (1–5, 11, 12), and basolateral membrane vesicles (BLMV) (12–14), mostly using citrate or succinate as substrates.

In BBMV, succinate uptake was found to be mediated with low affinity (K_m = ~1 mM) (5, 8, 12, 15). Studies on the pH dependence suggested that citrate is transported in its protonated divalent form (Cit^{-2}) (1, 2, 12), whereas succinate is transported either in its deprotonated (−2) or protonated (−1) form (11). In addition, it was shown that the −3 form of citrate (trivalent form, Cit^{-3}) inhibits transport of Cit^{-2} (11). Radiotracer studies revealed that the cotransport process exhibits a stoichiometry of 2–3 sodium ions/dicarboxylate molecule (2, 8, 16). On the other hand, experiments with a voltage-sensitive dye showed that the cotransport was electrogenic (14, 17), which favors a 3:1 stoichiometry.

In BLMV, succinate transport was pH-sensitive and with high affinity (K_m = ~10 μM; Refs. 12 and 13), and citrate uptake was hardly pH-sensitive (12), suggesting that both divalent and trivalent citrate can be transported. The functional differences between BBMV and BLMV transport suggest that there exist different transporter isoforms on the apical and basolateral sides. Also, a possible presence of a trivalent citrate transport system in the basolateral membrane of the proximal tubule cell line from opossum kidney was proposed (9).

Citrate transport in the proximal tubule is of considerable interest because it has several implications for the kidney function. Citrate is metabolized by the kidney via the intramitochondrial tricarboxylic acid cycle, and this process provides up to 10–15% of renal oxidative metabolism (18, 19). Urinary citrate is a potent inhibitor of calcium stone formation by chelating calcium and inhibiting precipitation of calcium and crystallization of calcium-oxalate crystals (20). Hypocitraturia is found in about half of patients with renal stone diseases (21). Low urinary citrate levels are found in many conditions associated with decreases either in intraluminal or intracellular pH in the proximal tubules (*i.e.* systemic acidosis) or with potassium depletion. These conditions are known to increase citrate reabsorption (6, 22, 23). Interestingly, hypocitraturia may be found without apparent cause (idiopathic), but the underlying mechanism is still undetermined (24).

cDNAs of Na^+-dicarboxylate cotransporters have recently been isolated from rabbit kidney (NaDC-1) (25), human kidney (hNaDC-1) (26), rat intestine (27), and rat kidney (28). Both the rabbit and human transporters can transport tricarboxylic acid cycle metabolites with low affinities (29, 30). The expression of these cloned cotransporters in *Xenopus* oocytes allowed kinetic analyses under steady-state and presteady-state conditions and, in contrast to vesicle studies, with excellent control of membrane potential, external milieu, and in some cases internal milieu. In the present paper, we report the characterization, using the two-microelectrode voltage-clamp technique, and the tissue distribution of a rat dicarboxylate transporter (SDCT1) that has been recently cloned in our laboratory by homology screening.

* This work was supported by the International Human Frontier Science Program Long-Term Fellowship (to X.-Z. C.) and by National Institutes of Health Grant DK43171 (to M. A. H.). The costs of publication of this article were defrayed in part by the payment of page charges. This article must therefore be hereby marked "*advertisement*" in accordance with 18 U.S.C. Section 1734 solely to indicate this fact.

The nucleotide sequence(s) reported in this paper has been submitted to the GenBank™/EBI Data Bank with accession number(s) AF058714.

‡ To whom correspondence should be addressed: Renal Division, Brigham and Women's Hospital, Harvard Institutes of Medicine, 77 Ave. Louis Pasteur, Boston, MA 02115. Tel: 617–525-5820; Fax: 617–525-5830; E-mail: mhediger@rics.bwh.harvard.edu.

[1] The abbreviations used are: BBMV, brush border membrane vesicle(s); BLMV, basolateral membrane vesicle(s); Cit^{-2}, divalent citrate; Cit^{-3}, trivalent citrate.

EXPERIMENTAL PROCEDURES

Isolation of the Rat SDCT1 Clone—Sprague-Dawley rat kidney cortex mRNA was reverse transcribed and used for polymerase chain reaction with a set of degenerative primers corresponding to the amino acids 35–40 and 142–137 of rabbit NaDC-1 (25). Polymerase chain reaction products were used to screen the cDNA library of a rat kidney cortex in the vector λgt10 at high stringency. A positive clone 2.4 kilobases in size was subcloned into the *Eco*RI site of the pBluescript vector and sequenced.

Oocyte Preparation—Stage V and VI oocytes were extracted from female *Xenopus laevis* frogs and prepared as described previously (31). Capped cRNA of rat SDCT1 was synthesized by *in vitro* transcription from cDNAs in pBluescript SK^-. Defolliculated oocytes were injected with 25–50 ng of cRNA or water at the same day or the following day after defolliculation and maintained in Barth's solution (88 mM NaCl, 10 mM HEPES, 1.8 mM $MgCl_2$, 1 mM KCl, 0.82 mM $CaCl_2$, 0.82 mM $MgSO_4$, and 0.33 mM $Ca(NO_3)_2$, pH 7.4 by Tris-base or HEPES) supplemented with 2.5 mM sodium pyruvate, 50 μg/ml gentamicin, 10 units/ml penicillin, and 10 μg/ml streptomycin at 18 °C.

In Situ Hybridization—Digoxigenin-labeled antisense and sense run-off transcripts were synthesized using a Genius kit (Boehringer Mannheim) from a linearized expression plasmid (pBluescript SK^-) containing the complete SDCT1 coding sequence, using T3 and T7 RNA polymerases, respectively. Transcripts were alkali-hydrolyzed to an average length of 200–400 nucleotides. *In situ* hybridization was performed on cryosections (10 μm) of fresh-frozen tissue as described previously (32). The hybridization buffer consisted of 50% formamide, 5× SSC, 2% blocking reagent (Boehringer Mannheim), 0.02% SDS, and 0.1% *N*-laurylsarcosine. Probe concentrations were ~200 ng/ml. Sections were immersed in slide mailers in hybridization solution and hybridized at 68 °C for 18–68 h. Sections were then washed three times in 2× SSC and for 2 × 30 min in 0.2× SSC at 68 °C. The hybridized labeled probes were visualized using anti-digoxigenin Fab fragments (Boehringer Mannheim) and 5-bromo-4-chloro-indolyl phosphate/nitroblue tetrazolium chloride substrate (32). Sections were developed in substrate solution for 20–44 h and then rinsed in 100 mM Tris, 100 mM NaCl, 1 mM EDTA at pH 9.5 and coverslipped with Vectashield (Vector).

Radiotracer Transport Measurements—Uptake experiments were performed 3–6 days following injection. 8–10 oocytes were incubated in 0.5 ml of modified ND96 Barth's solution (96 mM NaCl, 2 mM KCl, 1.8 mM $CaCl_2$, 1 mM $MgCl_2$, 5 mM HEPES, pH 5.5–9.5 by Tris-base or HEPES) containing specific tracer substrate ([^{14}C]citrate or succinate) and terminated by washing five times with the ice-cold Barth's solution containing 1 mM citrate. Individual oocytes were then dissolved in 250 μl of 10% SDS and mixed with 2.5 ml of scintillation mixture.

Electrophysiology—The two-microelectrode voltage-clamp technique was used to perform experiments in conjunction with a commercial amplifier (Clampator One, model CA-1B, Dagan Co., Minneapolis, MN). Solutions used for extracellular perfusion (at approximately 1.5 ml/min) contained 100 mM NaCl + choline-chloride, 10 mM HEPES, 2 mM KCl, 1.8 mM $CaCl_2$, 1 mM $MgCl_2$, 0–5 mM citrate, pH 5.5–9.5 by Tris-base or HEPES. For experiments using Cl^--free solutions, gluconate-(Na, K, Ca, Mg) was used to replace NaCl, KCl, $CaCl_2$ or $MgCl_2$, and an agar bridge, composed of 3 M KCl and 2% agar, was used to connect the bath solution with the grounding electrodes. After 5 min of membrane potential stabilization following microelectrode impalements, the membrane potential was clamped at the holding potential (V_h) of −50 mV. 90-ms voltage pulses between −160 and +60 mV were then applied, and steady-state currents were obtained by averaging signals 70–85 ms after initiation of voltage pulses. The substrate-evoked currents were evaluated as the difference between currents recorded before and after substrate addition. Experimental results were expressed in the form of mean ± S.E. (N), where N indicates the number of oocytes obtained from at least two different frogs. The curve-fitting procedures were performed using SigmaPlot (version 4.00, San Rafael, CA), and each fitted parameter is associated with an error that represents the error in the fitting estimates.

Determination of Charge to Tracer Uptake Ratio—One of the approaches to determine the Na^+ to citrate (or succinate) stoichiometry consists of simultaneously measuring citrate- or succinate-evoked currents and [^{14}C]citrate (or succinate) uptake under voltage-clamp conditions. Currents were monitored and recorded after an oocyte was clamped at −60 mV and perfused with substrate-free solution (control solution). The perfusion was stopped before adding to the chamber 10 μl of extracellular solution containing 20-fold concentrated cold and hot substrate. For measurements at pH 7.5, cold citrate and succinate were 20 and 2 mM, respectively. Upon substrate addition, the solution in the chamber was gently mixed until the substrate-evoked currents start to stabilize. After 4–5 min, washing was started by perfusing the oocyte with the control solution, and the current usually came back to the original base line. The oocyte was removed from the chamber for further washing with ice-cold extracellular solution containing 1 mM citrate before proceeding with scintillation counting. The charge moved during clamping was calculated by integrating the substrate-evoked current over the uptake period. If there was a slight base line shift during the uptake period, a linear shift was assumed. Charge was converted into pmol to compare with radiolabeled substrate uptake. The volume of the oocyte chamber was estimated to be about 200 μl; thus the final substrate concentration ([S]) in the chamber was approximately 20-fold diluted (*i.e.* ~1 mM citrate or ~0.1 mM succinate). Because cold and hot substrates were premixed, the ratio of specific current to the radiolabeled uptake will not be affected by spatial and temporal variations in substrate concentration within the chamber.

Thermodynamic Determination of Stoichiometry—This procedure consists of measuring the reversal potential (V_r), *i.e.* the membrane potential where the inhibitor-sensitive current is zero. In the present study, succinate was used as the substrate at 20 and 200 μM, and phloretin at 0.5 mM was used as the inhibitor. Because at pH 7.5 succinate is predominantly in its divalent (−2) form and assuming that n sodium ions are coupled to one succinate molecule, the relationship between V_r and succinate concentration ([Succinate]) at 22 °C is (33) as follows.

$$V_r = \frac{58.5\ \text{mV}}{n-2}\,\text{Log}\,\frac{[Na^+]_o^n[\text{Succinate}]_o}{[Na^+]_i^n[\text{Succinate}]_i} = \frac{58.5\ \text{mV}}{n-2}\,\text{Log}([\text{Succinate}]_o) + C \quad \text{(Eq. 1)}$$

where C is a constant if it is assumed that bilateral Na^+ and intracellular substrate concentrations remained unchanged during measurements. C can be eliminated when the V_r shift is determined by changing succinate from 20 to 200 μM.

Formulae Describing Inhibition of Cit^{-2} Transport by Cit^{-3}—Assuming that Cit^{-3} is a competitive inhibitor for Cit^{-2} (with an inhibition constant of K_i^{-3}) and that the Na^+:citrate stoichiometry is 3:1, the observed currents can be expressed as follows (34).

$$I = \frac{NeV_{max}^{-2}\cdot[Cit^{-2}]}{(1+[Cit^{-3}]/K_i^{-3})\cdot K_m^{-2}+[Cit^{-2}]} \quad \text{(Eq. 2)}$$

where, N and e indicate the number of transporters and the elementary charge, respectively, and [Cit^{-2}] and [Cit^{-3}] denote the concentrations of Cit^{-2} and Cit^{-3}, respectively. K_m^{-2} is the affinity constant for Cit^{-2}. The presence of SDCT1 might affect the protonation state of citrate during substrate-protein interaction. Assuming that citrate is either in its −2 or −3 form at pH ≥ 5.5 and that the equilibrium constant is K, then

$$[Cit^{-2}] = [H^+]\cdot[Cit]/(K+[H^+]) \text{ and } [Cit^{-3}] = K\cdot[Cit]/(K+[H^+]) \quad \text{(Eq. 3)}$$

where [Cit] is the concentration of citrate. Equation 2 can also be rewritten in the Michaelis-Menten form.

$$I = \frac{I_{max}^{Cit}\cdot[Cit]}{K_m^{Cit}+[Cit]} = \frac{I_{max}^{H}\cdot[H^+]}{K_m^{H}+[H^+]} \quad \text{(Eq. 4)}$$

where the affinity constant for citrate (K_m^{Cit}), and the maximal current for citrate (I_{max}^{Cit}) are functions of [H^+]:

$$\begin{cases} K_m^{Cit} = \dfrac{K_m^{-2}\cdot K_i^{-3}\cdot(K+[H^+])}{K_m^{-2}\cdot K + K_i^{-3}\cdot[H^+]} \\ I_{max}^{Cit} = \dfrac{N\cdot e\cdot V_{max}^{-2}\cdot K_i^{-3}\cdot[H^+]}{K_m^{-2}\cdot K + K_i^{-3}\cdot[H^+]} \end{cases} \quad \text{(Eq. 5)}$$

RESULTS

Sequence Homology and in Situ Hybridization—The SDCT1 clone encoded a 587-amino acid-residue protein that has 75% identity to the rabbit NaDC-1 (25) and 77% to the human kidney hNaDC-1 (26). During this study, rat intestinal and renal Na^+-dicarboxylate cotransporters were also identified (27, 28) and showed 98% amino acid identity to SDCT1 respec-

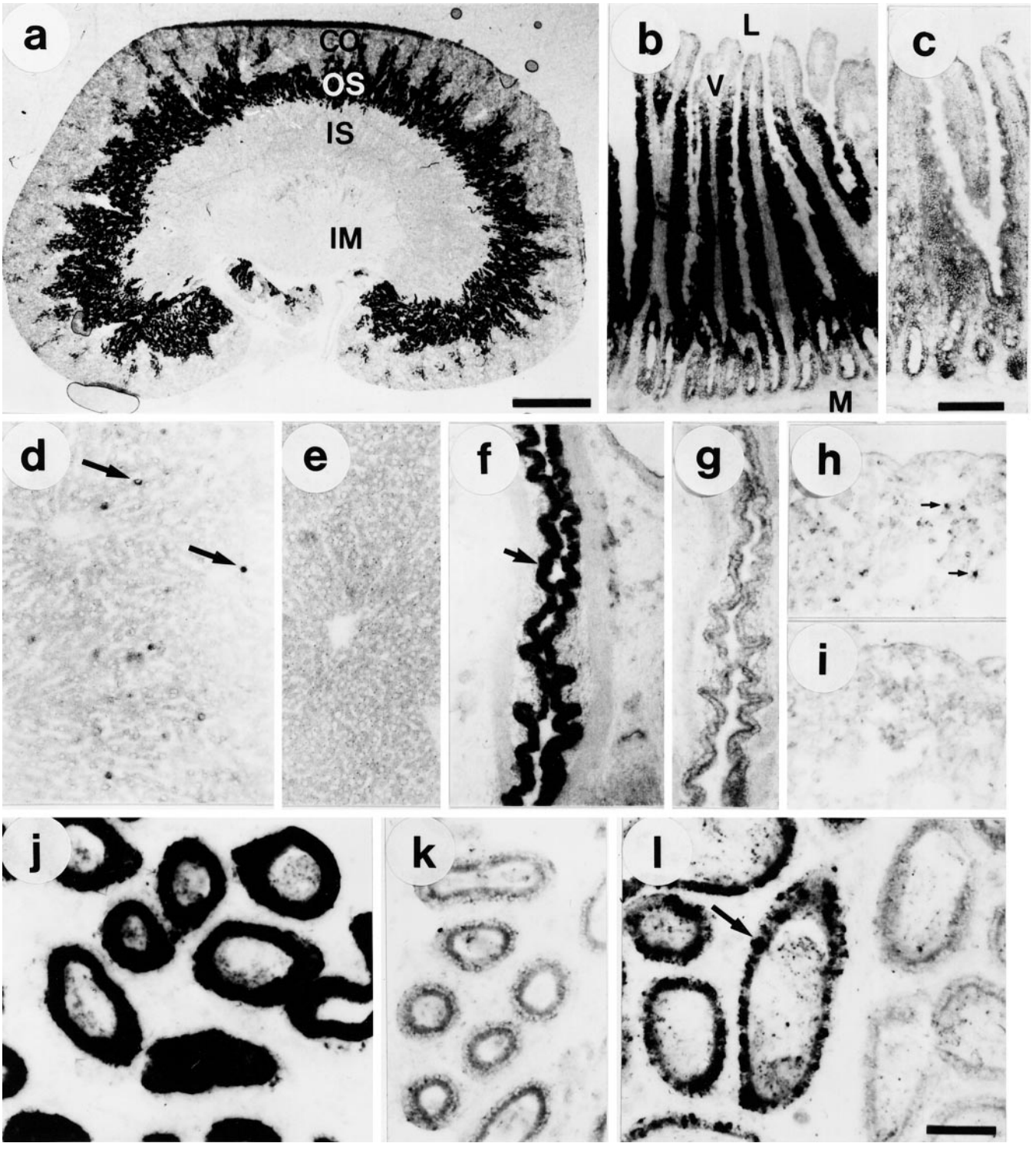

FIG. 1. **Distribution of SDCT1 mRNA in rat tissues as detected by nonradioactive *in situ* hybridization using digoxigenin-labeled cRNA probes.** *a*, in kidney, SDCT1 labeling displays the characteristic pattern of S3 proximal tubule segments in the outer stripe of outer medulla. *CO*, cortex; *OS*, outer stripe; *IS*, inner stripe; *IM*, inner medulla. *b*, in duodenum, SDCT1 is strongly expressed in enterocytes lining the intestinal villi. *M*, muscle layer; *V*, villus; *L*, lumen. *c*, control experiment shows the absence of labeling in duodenum with sense probe. *d*, in liver, SDCT1 is relatively strongly expressed by a small subset of cells (*arrows*). *e*, control experiment shows the absence of labeling in liver with sense probe. *f–i*, in lung, SDCT1 is expressed in cells of the bronchiole epithelium (*f*, *arrow*) and in cells of the alveolar epithelium (*h*, *arrows*). *g* and *i*, sense signals in bronchiole and alveolar epithelium. *j*, in epididymis, SDCT1 is strongly expressed in cells in the initial segment of the tubular epithelium. *k*, sense signal in epididymis initial segment. *l*, in the epididymis head, more proximal segments (*arrow*) of the tubular epithelium express moderate SDCT1 levels, whereas more distal segments express very low levels. *Bars*, 2 mm for *a*, 200 μm for *b* and *c*, and 100 μm for *d–l*.

tively. However, functional characterization of these proteins has not been reported. High stringency *in situ* hybridization experiments demonstrated that SDCT1 is predominantly localized in S3 segments of proximal tubules in the outer stripe of outer medulla (Fig. 1*a*) and in a small subset of tubular cells in the outer part of inner medulla (not shown). In duodenum, SDCT1 is strongly expressed by enterocytes lining the lower three-quarters of the intestinal villi but not in lower crypt cells (Fig. 1*b*). SDCT1 expression was also observed in ileum (not shown). In liver, a small subpopulation of cells, possibly hepa-

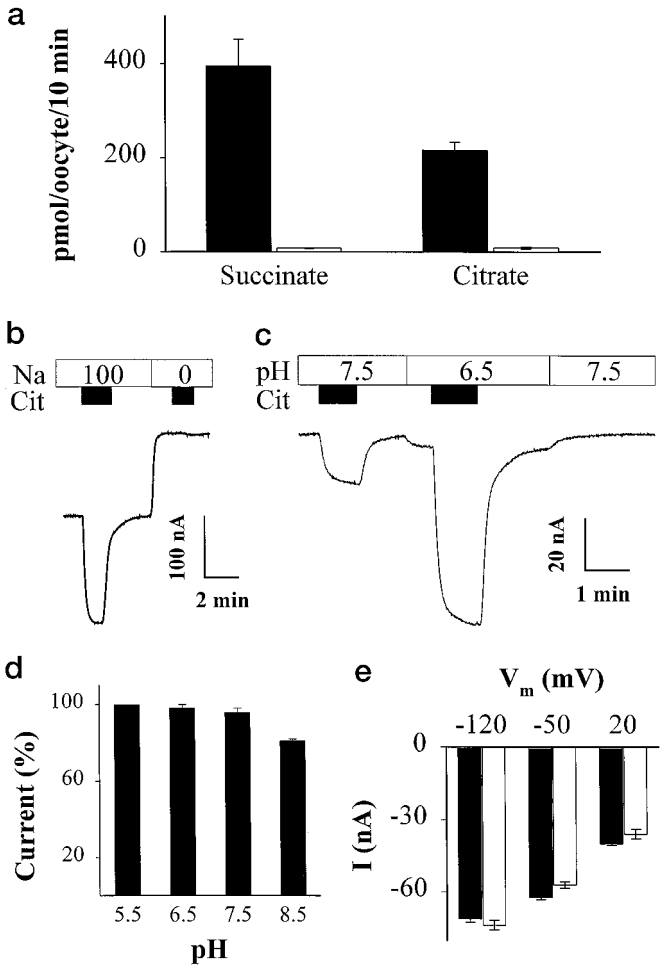

FIG. 2. **Citrate- or succinate-evoked cotransport under various conditions.** *a*, [^{14}C]succinate (0.1 mM) and citrate (1 mM) uptakes were measured and averaged from 8–10 SDCT1-injected (*filled bars*) and H_2O-injected (*open bars*) oocytes in each group. *b*, citrate-generated current was continuously recorded at the holding potential of −50 mV in the presence of 100 mM Na^+ or in the absence of Na^+. Application of citrate (2 mM) is indicated by *solid bars*. *c*, pH dependence of inward current generated by 200 μM citrate (solid *bars*) is demonstrated by superperfusing oocytes with solution at pH 7.5 or 6.5 (V_h = −50 mV). *d*, currents evoked by addition of 20 μM succinate were obtained at different pH and normalized to the current obtained at pH 5.5 (= 49.3 ± 2.8 nA, n = 3). *e*, Na^+-citrate cotransport currents were detected at different potentials in the presence (*filled bars*) or absence (*open bars*) of chloride.

tocytes, was strongly labeled for SDCT1 message (Fig. 1*d*). These SDCT1-positive cells did not form a particular pattern and were scattered throughout the liver. In lung, SDCT1 message was expressed by cells in the bronchiole epithelium (Fig. 1*f*) and by cells in the alveolar epithelium (Fig. 1*h*). Finally, SDCT1 mRNA was expressed in the tubular epithelium of epididymis: high levels of SDCT1 mRNA were present in epithelial cells in the initial segment and more moderate levels in proximal segments of the epididymis head (Fig. 1*j*). In more distal segments of epididymis head (Fig. 1*l*) or in segments of epididymis tail (not shown), SDCT1 labeling was negative.

Expression in Xenopus Oocytes—When mRNA of the SDCT1 was injected into *Xenopus* oocytes, 25- and 50-fold increases in [^{14}C]citrate and succinate uptakes were obtained, respectively, compared with H_2O-injected oocytes (Fig. 2*a*). Using the two-microelectrode voltage-clamp technique, SDCT1-mediated transport was shown to be electrogenic and sodium-dependent, as no significant currents were observed upon citrate addition when NaCl was substituted by choline-chloride (Fig. 2*b*). Citrate-evoked inward currents were pH-sensitive and stimulated by increasing the proton concentration in the solution (Fig. 2*c*). In contrast, succinate-evoked cotransport was not pH-sensitive between pH 5.5 and pH 7.5, although it was slightly reduced at pH 8.5 (Fig. 2*d*). Because succinate has a pK value (pK2) of 5.6, these data suggest that it can be transported either in its −1 or −2 form. When chloride was replaced by gluconate, no remarkable difference in current was observed at various potentials (Fig. 2*e*), demonstrating that SDCT1-mediated transport is chloride-independent.

Ion and Substrate Specificity—In addition to sodium, potassium can also drive substrate transport. At −50 mV, 50 mM K^+, and pH 7.5, 1 mM citrate stimulated currents averaging 20 ± 3% (n = 5) of those evoked in the presence of 100 mM Na, under the same conditions. In contrast, when 1 mM succinate was used in place of 1 mM citrate, the K^+-coupled current was only 10% of the Na^+-coupled current, and no detectable currents were observed with 50 μM succinate. These data indicate that K^+ couples to substrates with a lower efficiency than Na^+. When 1 mM citrate or 50 μM succinate was added to solution containing 100 mM Li^+ in place of Na^+, no detectable currents were stimulated, indicating that lithium cannot drive SDCT1-mediated cotransport. In fact, lithium had a significant inhibitory effect. In the presence of 50 μM succinate, when 3 mM Li^+ was added to solutions containing 100 and 20 mM Na^+, the Na^+-coupled currents were reduced to 50 ± 2 and 28 ± 1% (n = 3), respectively. Because higher Li^+ inhibition was observed at lower Na^+ concentration, these data suggest that Li^+ can compete with Na^+ for binding but is not itself translocated.

Currents evoked by citrate addition were voltage-dependent (Figs. 3*a* and 4*a*). At −50 mV and pH 7.5, the apparent affinity for citrate was 0.64 ± 0.01 mM (n = 5) (Fig. 3*b*). Currents elicited by application of substrates (1 mM) to the same oocytes ranked in the following order: fumarate > L-malate > succinate > α-ketoglutarate > oxaloacetate > citrate > L-aspartate > L-glutamate > D-aspartate > D-glutamate (Fig. 3*d*). On the other hand, neutral and positively charged amino acids, maleic acid, amiloride, dimethylsuccinate, furosemide, and monocarboxylates (L-lactate, pyruvate, nicotinate, acetoacetate, and γ-hydroxybutyrate), all at 1 mM levels, did not evoke detectable currents (V_h = −50 mV). Likewise, these substances had no inhibitory effects on 1 mM citrate-evoked currents, which is similar to results obtained from tracer measurements for human NaDC-1 (29). These results indicate that monocarboxylates are not transported by SDCT1. The Krebs cycle metabolites succinate, α-ketoglutarate, and oxaloacetate stimulated SDCT1-mediated currents with high affinities and high efficiencies, whereas both L-/D-glutamate and aspartate generated currents with low affinities and low efficiencies (Table I).

The apparent affinity constant for sodium was 19.5 ± 0.7 mM, and the Hill coefficient (n_H) was 2.07 ± 0.09 (n = 6) at 2 mM citrate, V_h = −50 mV, and pH 7.5 (Fig. 4*b*). This suggests that at least 2 sodium ions are coupled to each citrate molecule. In 4 oocytes from different batches, the maximal current for sodium (I_{max}^{Na}) increased about 3-fold upon hyperpolarization from 0 to −160 mV, and the apparent affinity constant for sodium (K_m^{Na}) decreased 50% from −40 to −160 mV (Fig. 4*c*).

Proton Dependence of Citrate and Glutamate Transport—At −50 mV, the apparent affinity for citrate increased about 10-fold to 57 ± 8 μM (n = 4) when pH decreased from 7.5 to 5.5 (Fig. 3, *b* and *c*). These observations are consistent with previous findings on rabbit and human NaDC-1 (29) and renal membrane vesicles (2, 11). In contrast, succinate-evoked currents were pH-independent (Fig. 2*d*). The proton affinity constant (K_m^H) was determined at [Cit] = 1 mM (Fig. 5*a*) and averaged 62 ± 14 nM (corresponding to pH 7.2 ± 0.1) from 3

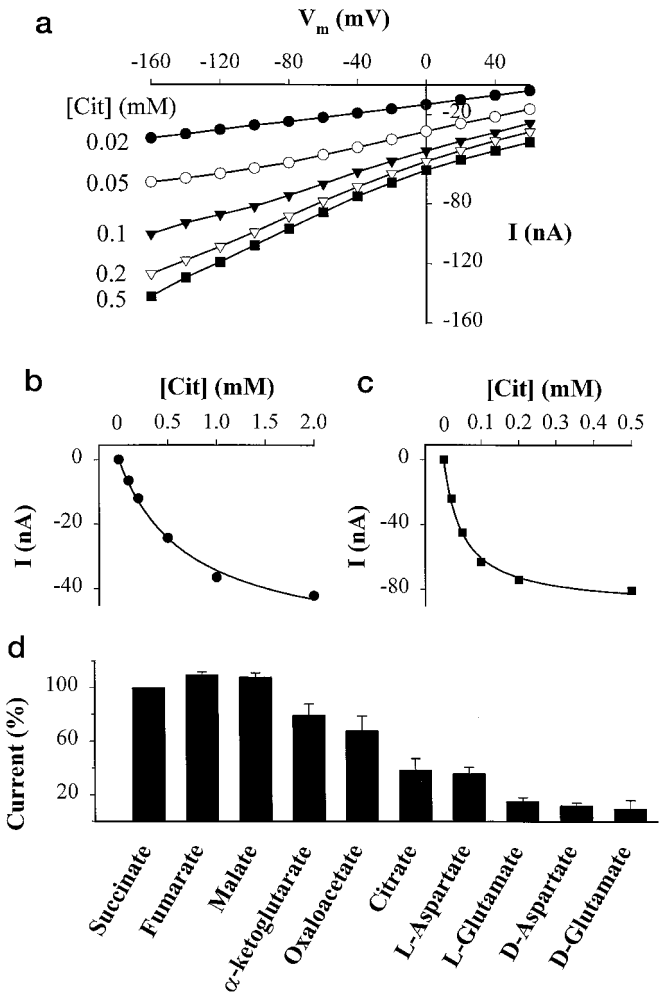

FIG. 3. **I-V curves of citrate-evoked currents and pH dependence of the apparent affinity constants and maximal currents for citrate.** *a*, currents due to addition of citrate ranging from 0.02 to 0.5 mM at pH 5.5 were plotted against the membrane potential. *b*, concentration dependence of SDCT1-mediated currents at $V_h = -50$ mV and pH 7.5. For these representative data, a Michaelis-Menten fit (Equation 4) gave $K_m = 0.70 \pm 0.10$ mM and $I_{max} = -58.6 \pm 3.4$ nA. The average K_m was 0.64 ± 0.01 ($n = 5$). *c*, currents recorded at pH 5.5 yielded $K_m = 49 \pm 4$ μM and $I_{max} = -90.6 \pm 2.4$ nA. *d*, to obtain the substrate specificity, currents due to application of various substrates at 1 mM were compared in the same oocytes ($n = 3–8$).

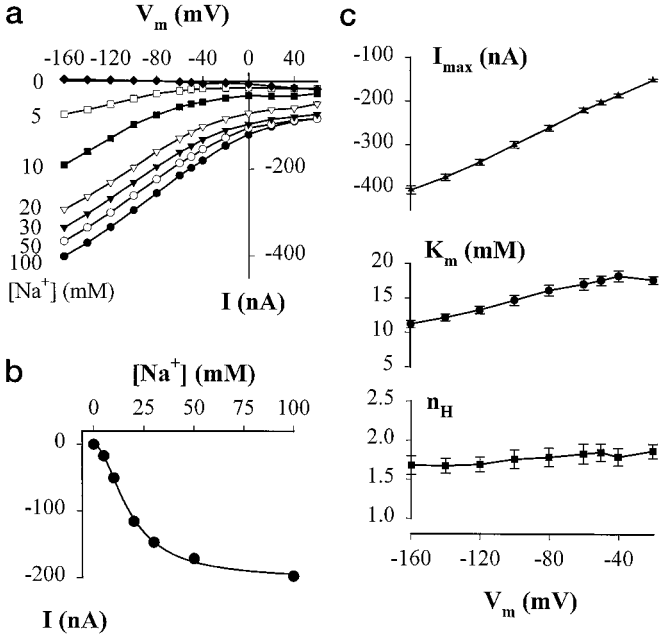

FIG. 4. **Sodium dependence of SDCT1-mediated currents at pH 7.5.** *a*, I-V curves at various [Na^+] were obtained as the difference between currents before and after application of 2 mM citrate. *b*, at −50 mV, the sigmoidal relationship of the cotransport current *versus* [Na^+] was fitted to the following Hill equation

$$I = \frac{I_{max} \cdot [S]^{n_H}}{(K_m)^{n_H} + [S]^{n_H}} \quad \text{(Eq. 6)}$$

yielding $K_m^{Na} = 17.6 \pm 0.7$ mM, $n_H = 1.9 \pm 0.1$, and $I_{max}^{Na} = 202 \pm 4$ nA. The averaged K_m^{Na} and n_H from 6 oocytes were 19.5 ± 0.7 mM and 2.07 ± 0.09, respectively. *c*, voltage dependence of K_m^{Na}, n_H, and I_{max}^{Na} was obtained by fitting the data shown in *panel a* to the Hill equation.

TABLE I
Substrate specificity of SDCT1

Substrate affinity constants (K_m) and maximal currents (I_{max}) were measured under voltage-clamp conditions ($V_h = -50$ mV). The ratio I_{max}/K_m is equal to the initial slope of the current versus [S] curve and indicates the transport efficiency of a substrate. Solution contained 100 mM Na^+, and the pH was 7.5. Averages were obtained from 3–8 oocytes.

Substrate	K_m	I_{max}/K_m
		nA/mM
Succinate	24 ± 2 μM	4410 ± 1147
α-Ketoglutarate	45 ± 6 μM	1893 ± 376
Oxaloacetate	53 ± 11 μM	1508 ± 241
Citrate at pH 5.5	57 ± 8 μM	1299 ± 210
Citrate	0.64 ± 0.01 mM	105 ± 17
L-Aspartate	1.9 ± 0.4 mM	77 ± 15
L-Glutamate	5.5 ± 0.6 mM	21 ± 3
D-Aspartate	18 ± 5 mM	18 ± 5
D-Glutamate	11 ± 3 mM	12 ± 7

oocytes. The pH dependence of the [^{14}C]citrate uptake was also determined and exhibited a Michaelis-Menten relationship with a similar K_m^H value (pH 7.2 ± 0.3, see Fig. 5*b*). The uptake vanished at high pH, indicating that trivalent citrate was not remarkably transported. Because proton translocation is not associated with transport of succinate (and other Krebs cycle intermediates, *e.g.* α-ketoglutarate) (data not shown), protons are unlikely to be coupling ions for citrate uptake. We propose that protons serve to protonate the trivalent form of citrate and that the divalent form is the predominant form transported.

For pH ≥ 5.5, citrate is both in the Cit^{-2} and Cit^{-3} form, and their relative proportion in solution is described by the equilibrium constant pK_3 (= 6.4). If Cit^{-3} had no effect on Cit^{-2} transport, then we would expect to have the same maximal currents for citrate (I_{max}^{Cit}) at different pH. However, measurements performed in the same oocytes revealed that I_{max}^{Cit} at pH 5.5 was 70% higher than I_{max}^{Cit} at pH 7.5 (see example in Fig. 3), indicating that Cit^{-3} inhibits Cit^{-2} transport. If inhibition was noncompetitive, currents at high substrate or proton concentrations would be expected to decrease (34). If inhibition was uncompetitive, the current as a function of [H^+] would be expected to be sigmoidal and to drop at high substrate concentrations. Because both of these predictions are not supported by our data, it is reasonable to assume competitive inhibition of Cit^{-2} transport by Cit^{-3}. Under this assumption and using Equation 5, we found that $K = 1.0 \pm 0.1$ μM, which corresponds to a pK value of 6.0 ± 0.1, $K_m^{-2} = 33 \pm 4$ μM and $K_i^{-3} = 1.5 \pm 0.2$ mM ($n = 3$). The obtained pK value is close to pK_3 of citrate, indicating that citrate protonation is likely to be determined by bulk solution. This result shows that the apparent affinity constant for divalent citrate is in fact high and close to K_m for (total) citrate at pH 5.5 and that the trivalent citrate is a relatively low efficiency inhibitor. Because divalent citrate is equivalent to a dicarboxylate in terms of the number of negative charges, our data show that SDCT1 transports only dicarboxylates.

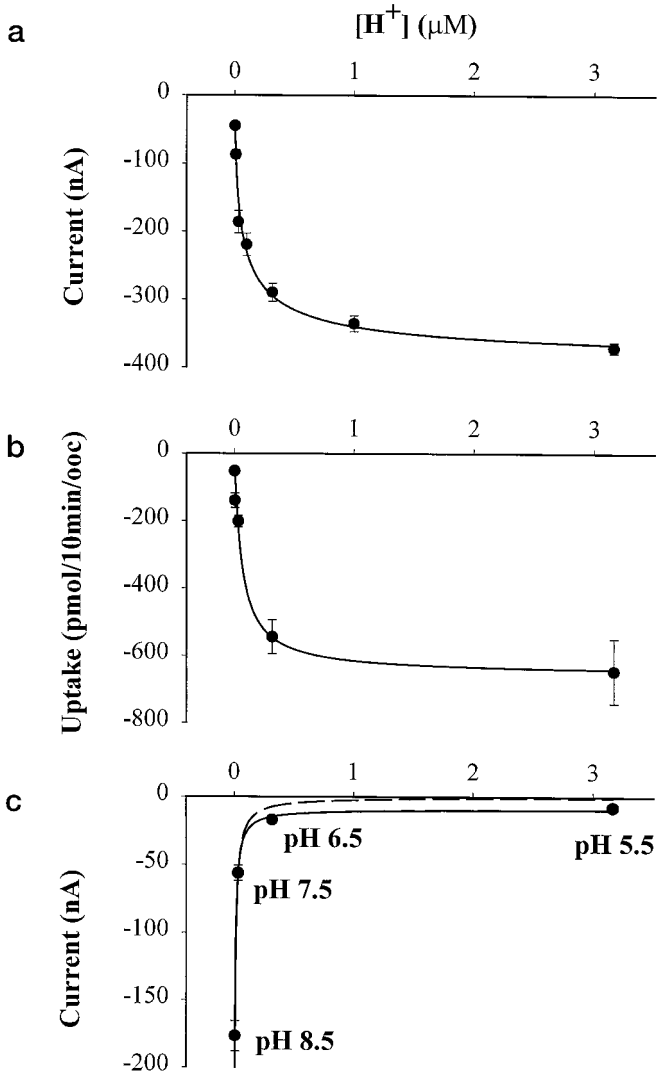

FIG. 5. **H^+ sensitivities obtained from current and/or tracer measurements.** *a*, under voltage-clamp conditions (V_h = −50 mM, 1 mM citrate), average currents (for pH from 5.5 to 8.5 with increment of 0.5) obtained from 3 oocytes were fitted to the Hill equation with K_m^H = 59.7 ± 16.7 nM (corresponding to pH 7.3 ± 0.3), n_H = 0.67 ± 0.08, and I_{max}^H = −392 ± 21 nA. *b*, [^{14}C]citrate uptakes at 1 mM level were obtained and averaged from 8–10 oocytes at each pH value (from 5.5 to 9.5 with increment of 1.0). From the Michaelis-Menten fit, K_m^H = 62 ± 20 nM (or pH 7.2 ± 0.3) and I_{max}^H = 653 ± 46 pmol/10 min/oocyte. *c*, currents evoked by 2 mM L-glutamate at pH 5.5, 6.5, 7.5, and 8.5 are illustrated. The *solid line* represents the Michaelis-Menten fit plus a constant *c* with K_m^H = 8.1 ± 2.4 nM (or pH 8.1 ± 0.3), I_{max}^H = −233 ± 20 nA, and *c* = −9.0 ± 4.6 nA. The *dashed line* is the best fit assuming that only the −2 form of glutamate is transported ($I = I_{max} \cdot K_m^H/(K_m^H + [H^+])$, with K_m^H = 10.8 ± 2.7 nM (or pH 8.0 ± 0.2) and I_{max}^H = −228 ± 18 nA.

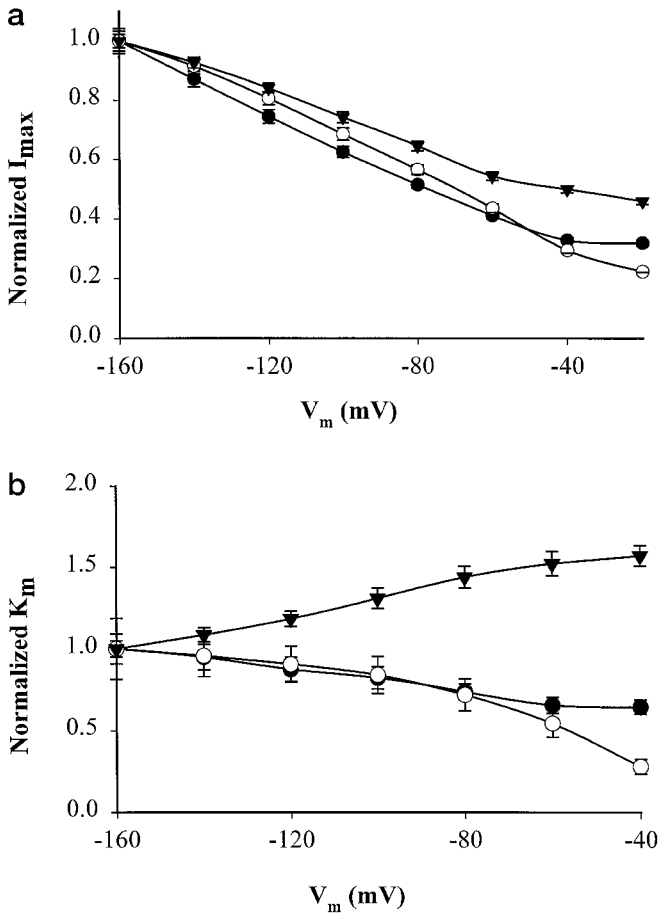

FIG. 6. **Voltage dependence of maximal currents and affinity constants.** *a*, maximal currents were normalized to I_{max} at −160 mV. The maximal current for citrate (I_{max}^{Cit}, , = −361 nA at −160 mV) was obtained at 100 mM Na^+ and pH 7.5. The maximal current for proton (I_{max}^H, ○, = −225 nA at −160 mV) was obtained at 100 mM Na^+ and 1 mM citrate. The maximal current for sodium (I_{max}^{Na}, ▼, = −404 nA at −160 mV) was obtained at 2 mM citrate and pH 7.5. *b*, affinities were obtained in the same oocytes used to determine I_{max} shown in *a* and were normalized to K_m at −160 mV. In this example, the affinity constants at −160 mV for citrate, proton, and Na^+ were 1.07 mM, 116 nM (or pH 6.94), and 11.2 mM, respectively.

Interestingly, glutamate transport exhibited a pH dependence opposite to that of citrate transport. Currents resulting from addition of 2 mM L-glutamate at pH 7.5, 6.5, and 5.5 represented 31.8, 9.6, and 4.4% of that at pH 8.5 (Fig. 5*c*). Because glutamate has a pK_2 of 9.67 for the amino group, this result indicates that glutamate is largely transported in its −2 form (Glu^{-2}) and that the affinity for Glu^{-2} is in fact high. However, if only the −2 form was transported, we would predict, based on the Michaelis-Menten fit (*dashed curve* in Fig. 5*c*), a much lower current at pH 6.5 and no current at pH 5.5, contrary to the observed data (*solid circles* in Fig. 5*c*). This suggests that the predominant −1 form is also transported, although at a much lower transport rate. The pH dependence of glutamate and citrate transport supports our concept that protons affect SDCT1-mediated transport through substrate protonation or deprotonation. Selective transport of either Cit^{-2} or Glu^{-2} would result in pH changes on both *trans* and *cis* sides of the membrane.

Voltage-dependent Steps—To obtain information on the voltage dependence of individual steps, we determined maximal currents I_{max} as a function of membrane potential. At high Na^+,H^+ and substrate concentration, the binding processes are fast enough so that translocation of the loaded transporter or relocation of the free transporter across the membrane becomes rate-limiting and determines I_{max}. We determined the voltage dependence of I_{max} for citrate, sodium, and proton (Fig. 6*a*), all of which exhibited a 3-fold increase upon hyperpolarization of V_m from −20 to −160 mV. This indicates that translocation of either the loaded or the free transporter or both are voltage-dependent.

To gain insight into the voltage dependence of the Na^+,H^+ and substrate binding processes, we plotted the apparent affinity constants K_m as a function of V_m (Fig. 6*b*). The citrate affinity decreased with hyperpolarization, which is consistent with unfavorable binding of negative charge at hyperpolarized V_m. The sodium affinity increased with hyperpolarization, consistent with preferred binding of positive charge at negative

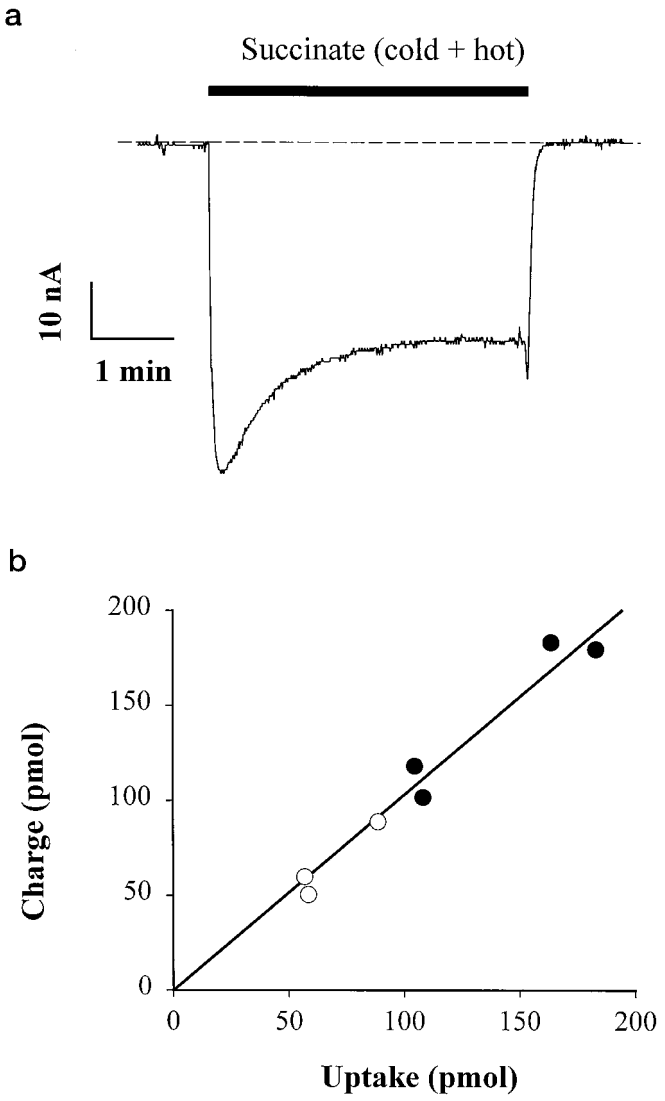

FIG. 7. **Stoichiometry determination using simultaneous measurements of substrate-evoked currents and tracer uptakes under voltage-clamp conditions (V_h = −60 mV).** *a*, representative example of currents generated by 100 μM succinate (cold + hot). The charge moved was calculated by integrating the succinate-evoked current over the uptake period. *b*, the charge moved was converted to pmol and plotted against uptake. For experiments using succinate ( ) the incubation time was 5 min, whereas for those using citrate (○) the incubation time was 4 min. When both data are plotted together, the slope of the linear fit, which is equal to the charge:uptake ratio, is 1.03 ± 0.03.

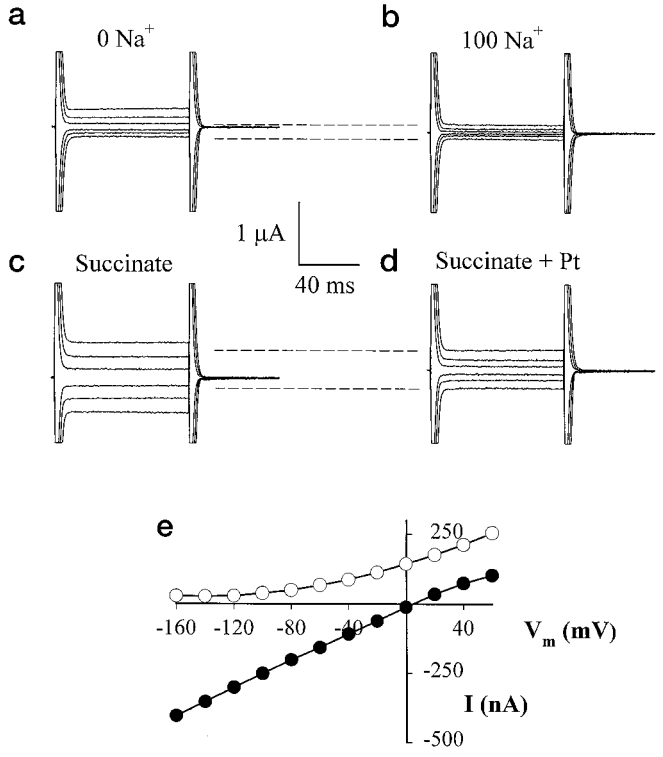

FIG. 8. **Na^+ and phloretin effects on SDCT1-specific currents.** *a*, time course of transmembrane currents recorded in the absence of external Na^+ upon voltage jumps from V_h of −50 mV to final potentials ranging between −160 and +60 mV, each separated by 20 mV. For clarity, only currents corresponding to V_m of −160, −120, −80, −20, +20, and +60 mV are shown. *b*, currents at 100 mM extracellular Na^+ were recorded with the same oocyte as in *a*. Outward currents at positive potentials were inhibited by Na^+ addition. *c*, currents were obtained in the presence of 200 μM succinate and 20 mM extracellular Na^+. *d*, both inward and outward currents were inhibited by application of 0.5 mM phloretin (*Pt*) to the same oocyte as in *c*. *e*, currents inhibited by Na^+ and phloretin were obtained as the difference between those shown in *a* and *b* (*open circles*) and between those in *c* and *d* (*solid circles*), respectively.

V_m. Interestingly, despite the positive charge of H^+, its affinity had the same V_m dependence as that of citrate. This paradoxical V_m dependence can be explained if H^+ and Cit^{-3} react to form Cit^{-2} before being transported, resulting in a proton-binding affinity that is characterized by binding of the negatively charged Cit^{-2}. Thus H^+, unlike Na^+, is likely not a coupling ion but serves to protonate citrate before binding to the transporter.

Charge:Uptake Ratio—We measured the citrate or succinate-evoked current under voltage-clamp conditions and, at the same time, [^{14}C]citrate or [^{14}C]succinate uptake (see "Experimental Procedures"). The charge moved during uptake is equal to the time integral of the current (Fig. 7*a*). At pH 7.5, the charge:uptake ratio in the presence of 1 mM [^{14}C]citrate was found to be 0.97 ± 0.06, averaged from 3 oocytes. In the presence of 0.1 mM [^{14}C]succinate, the ratio averaged 1.04 ± 0.05 from 4 oocytes. When combining the data from all measurements, a linear fit with a slope (charge:uptake ratio) equal to 1.03 ± 0.03 was obtained (Fig. 7*b*). At pH 7.5, succinate is mainly in its −2 form, and our data presented above showed that citrate is also transported in its −2 form. It follows that both the sodium:citrate and the sodium:succinate stoichiometries are 3:1 for SDCT1.

Inhibition of SDCT1 Transport and Reversal Potentials—In oocytes expressing SDCT1 but not in H_2O-injected oocytes, external Na^+ in the absence of external substrate inhibited outward currents at positive potentials (Fig. 8, *a*, *b*, and *e*). These SDCT1-specific outward currents are likely to correspond to the reversed transport generated by intracellular dicarboxylates. In contrast, succinate (200 μM) or citrate (2 mM) did not significantly inhibit outward currents in the absence of extracellular Na^+ (see *curve* corresponding to 0 Na^+ in Fig. 4*a*). Phloretin (0.5 mM) inhibited both inward and outward currents obtained in the presence of 20 mM external Na^+ and 200 μM succinate (Fig. 8, *c*, *d*, and *e*) with an estimated inhibition constant (K_i) of 40 μM at −50 mV. No significant phloretin-inhibitable currents were detected in H_2O-injected oocytes. In the absence of external substrate but in the presence of sodium, a small phloretin-inhibitable inward current (at $V_m < -90$ mV, Fig. 9) along with a phloretin-inhibitable outward current (at $V_m > -90$ mV) was observed. This indicates that an SDCT1-mediated uncoupled sodium leak exists and that at least one sodium ion binds first to the transporter. Thus, the small currents at $V_m < -100$ mV in Fig. 8*e* (*open circles*) arise from

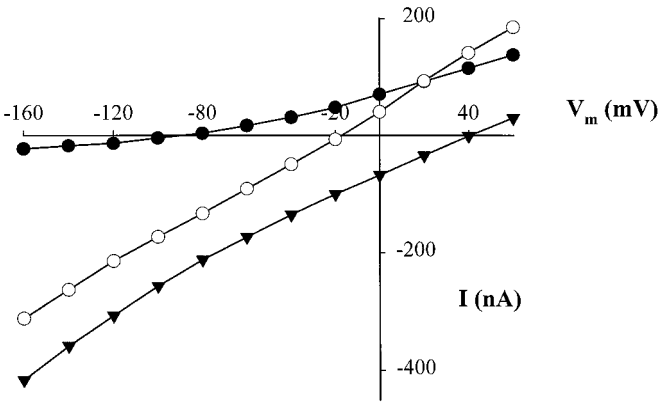

FIG. 9. **Phloretin-sensitive currents *versus* V_m at different external succinate concentrations.** [Phloretin] = 0.5 mM and [Na^+] = 20 mM. In the absence of external substrate ( ), phloretin inhibited an inward sodium leak with a reversal potential equal to −91 mV. When 20 μM succinate was applied, V_r shifted to −17.5 mV. Between 20 (○) and 200 μM (▼) external succinate, the V_r shift was 57.5 mV in this example.

both the SDCT1-specific sodium leak and SDCT1-independent sodium currents.

Determination of the Stoichiometry Using the Thermodynamic Method—Upon external addition of 20 or 200 μM succinate, the phloretin-sensitive currents exhibited reversal potentials V_r that shifted toward more positive potentials (Fig. 9). The effects of phloretin on SDCT1 are similar to that of phlorizin on the high affinity Na^+-glucose cotransporter SGLT1 expressed in oocytes (31, 33, 35, 36). From 20 to 200 μM succinate, the V_r shift averaged 54.5 ± 1.9 mV (n = 4), which is equivalent to an n value of 3.08 ± 0.04 (see Equation 1). This value confirms the result from tracer determinations that the sodium:substrate stoichiometry is 3:1.

Significance of SDCT1-mediated Uncoupled Sodium Currents—In the absence of external substrate and at 20 μM succinate, reversal potentials obtained from phloretin-inhibited currents averaged −85 and −4 mV, respectively. From these data, the characteristic constant K_c that quantitatively describes the significance of the sodium leak with respect to the cotransport current (33) can be estimated to be 1 μM. When [Succinate] = K_C, the Na^+-succinate cotransport current is equal to the uncoupled sodium leak current (33). This means that the sodium leak is small and equivalent to the current generated by 1 μM succinate. Because K_m for succinate is 24 μM, the sodium leak in the absence of extracellular substrate represents approximately 4% of the maximal current for succinate (see Equation 3 in Ref. 37). At low substrate concentration (comparable with its K_c), SDCT1 does not function in the proper coupling mode because of the sodium leak. At [S] ≫ K_c, where the leak is negligible (33), the sodium:substrate coupling is stoichiometric.

DISCUSSION

Localization—In the present study, we have described a high affinity Na^+-coupled dicarboxylate transporter, SDCT1, from rat kidney, its localization, and a number of biophysical characteristics. Our *in situ* hybridization studies demonstrated that SDCT1 is localized in the late portion of proximal tubules (S3 segments). Previous studies using membrane vesicles prepared from renal cortex revealed low affinity transport in BBMV (K_m for succinate = ~1 mM) and high affinity transport in BLMV (K_m for succinate = ~10 μM). In BBMV, citrate but not succinate transport was highly dependent on extracellular pH. In BLMV, extracellular pH had a remarkable effect on succinate and methylsuccinate uptake but little effect on citrate uptake (12, 13). In the present study, using oocytes expressing SDCT1, succinate transport was with high affinity and pH-independent (Fig. 2*d*), and citrate transport increased about 4-fold when pH was decreased from 8.5 to 5.5 (Fig. 5). Thus, the pH dependence of SDCT1-mediated transport suggests that SDCT1 is an apical transporter. It is possible that the previously studied low affinity system in BBMV has a high capacity and masked the high affinity transport of SDCT1 in S3 segments. In fact, tubule perfusion studies in rabbit kidney indicated that dicarboxylate reabsorption occurs in S3 segments with low capacity compared with the early part (*i.e.* S1 segments) (10, 38). It is likely that high affinity low capacity SDCT1 participates in final reabsorption of dicarboxylates that escape the early part of proximal tubules where the low affinity transporters rabbit and human NaDC-1 are expected to be expressed (25, 26). Similar situations have been demonstrated for the reabsorption of other solutes such as glucose.

The strong expression of SDCT1 mRNA in the small intestine supports the view that it plays an important role in intestinal absorption of dietary dicarboxylates, including citrate and other Krebs cycle intermediates. Absorbed citrate is mainly utilized in the liver and the kidney, but little is known about metabolism in other organs. In the initial segment of the epididymis, SDCT1 mRNA message and the citrate and glutamate levels are high (39, 40). Based on micropuncture studies, glutamate concentrations reach 50, 20, and 0.5 mM in the initial (caput), middle (corpus), and distal (cauda) segments of the epididymis, respectively (39). This massive glutamate decrease is paralleled by a decrease in luminal Na^+ concentration (110, 60, and 20 mM in caput, corpus, and cauda, respectively), glutamate transport activity, and γ-glutamyl transpeptidase levels (39, 41) (γ-glutamyl transpeptidase may partially provide glutamate by hydrolyzing glutathione). These distributions are in good agreement with that of SDCT1 mRNA in epididymis, suggesting the involvement of SDCT1 in contributing to the low pH environment in the head of the epididymis and the nutritional needs of sperms.

Selectivity of Driving Cations—Based on the observed K^+–dependent SDCT1-mediated currents and on the Li^+-inhibited sodium currents, we have suggested that both K^+ and Li^+ can compete with Na^+ for binding to SDCT1. Similar interactions between monovalent cations were reported previously in SGLT1 where both Li^+ and H^+ can be driving ions (42). In the amino acid transporter KAAT1 cloned from lepidopteran insect larvae, both Na^+ and K^+ are good driving ions (43). This might be due to a similarity in ionic structure among monovalent cations. K^+ at 2 mM did not drive any significant currents in the absence of Na^+ (Fig. 4*a*). Also we did not observe any difference in 100 mM Na^+-coupled currents between solutions with or without 2 mM K^+. In contrast, because intracellular K^+ concentrations, under physiological conditions, are much higher than intracellular Na^+ concentrations ($[Na^+]_i$), the K^+-coupled reversed transport might significantly contribute to the observed outward currents mediated by SDCT1. SDCT1 might provide an important dicarboxylate exit pathway through reversed transport.

Stoichiometry—Previous vesicle studies indicated a sodium: substrate stoichiometry of 2:1 to 3:1. For SDCT1, a 3:1 stoichiometry was obtained using both the voltage-clamp tracer method and the thermodynamic method. The voltage-clamp condition was critical in these stoichiometry studies to accurately determine specific charge accumulation in oocytes. Currents were continuously recorded during the entire radioisotope uptake. This is important as currents remarkably change during uptake (Fig. 7*a*). The 3:1 stoichiometrical ratio has physiological implications. Firstly, it can create higher dicar-

boxylate gradients across the cell membrane than a 2:1 coupling mechanism. Secondly, the 3:1 stoichiometry of dicarboxylate transport results in an electrogenic transport that can utilize the existing membrane potential as a driving force for substrate accumulation. The high stoichiometry and high affinity ensure efficient reabsorption of trace amounts of dicarboxylates that escaped the early proximal kidney tubules.

Inhibition of SDCT1-mediated Currents—In oocytes expressing SDCT1, addition of 100 mM Na^+ without external substrate evoked a large inward current (~120 nA; Fig. 2*b*). This current is SDCT1-specific because H_2O-injected oocytes only showed small currents (less than 20 nA). The current is not a sodium leak because 1) the total conductance of the oocyte at 100 mM Na^+ is lower than that in the absence of Na^+ and 2) the current amplitude decreased with hyperpolarization (Fig. 8, *a*, *b*, and *e*). This indicates that addition of 100 mM Na^+ reduces outward currents at positive membrane potentials (*trans*-inhibition). *Trans*-inhibition by Na^+ was also observed for sodium-dependent succinate transport in renal BBMV (4). The small currents at $V_m < -120$ mV may be attributed to the SDCT1-mediated sodium leak and SDCT1-independent sodium fluxes. Phloretin (as well as Li^+) were found to inhibit both inward and outward currents mediated by SDCT1 (Fig. 8, *c* and *d*). At −50 mV and without external substrate, the phloretin-sensitive SDCT1 currents were generally outwardly directed with an V_r average of −85.3 mV. This observation validates the concept that Na^+ inhibits SDCT1-specific outward currents.

Endogenous SDCT1 Substrates in Xenopus Oocytes—The V_r values can be used to estimate the concentration of intracellular substrate for SDCT1 in oocytes. Assuming that $[Na^+]_i$ is 10 mM (44) and using Equation 1, the intracellular substrate concentration is equivalent to ~100 μM succinate. If all of the intracellular substrate was citrate, this would be equivalent to an endogenous citrate concentration in the mM range, the same order of magnitude as in the renal tissue (45).

Substrate Binding Order and Kinetic Model—Although it is well established now that 3 sodium ions are stoichiometrically coupled to one substrate molecule, the order by which these 3 sodium ions and the substrate bind to SDCT1 remains to be resolved. Assuming that Na^+ and substrate bind to the protein in an orderly fashion, there are four possibilities: SNNN, NSNN, NNSN, and NNNS, where N = Na^+ and S = substrate. The presence of a phloretin-inhibitable sodium leak indicates that sodium ions bind before the substrate, eliminating SNNN. On the other hand, because external Na^+ alone but not external substrate alone *trans*-inhibits outward currents, this suggests that Na^+ and not substrate binds last to SDCT1, as can be explained by the King and Altman algorithm: in the absence of external Na^+, NNNS (but not NNSN or NSNN) predicts a term containing $[S]_o$ in the denominator of the expression for the outward current (I_o) (34, 46). When $[S]_o$ is high, I_o will decrease (*i.e.* I_o is *trans*-inhibited by $[S]_o$), which contradicts our experimental observation. In contrast, using the above algorithm, both NNSN and NSNN predict a *trans*-inhibition by $[Na^+]_o$ in the absence of external substrate, as observed, because $[Na^+]_o$ appears in the denominator of the expression for I_o. On the other hand, if the substrate was the last to bind, then the electroneutral exchange between external tracer substrate and internal cold substrate would be expected to be remarkable, resulting in an underestimation of charge to substrate uptake ratio, even under voltage-clamp conditions. However, the stoichiometry obtained by the tracer method was the same as that obtained by the thermodynamic method. Thus, our data are consistent with the models where the binding order for SDCT1 is NNSN or NSNN (Fig. 10).

Pathophysiological Implications—The importance of dicarboxylate reabsorption in the proximal tubules has been emphasized as the major determinant of urinary excretion of citrate, the potent inhibitor of calcium salt crystallization (20, 38). Hypocitraturia is therefore an important risk factor for kidney stone formation. Among many factors modulating renal citrate excretion, the most important is systemic acid-base status and K^+ depletion (6). In metabolic alkalosis, proximal tubular citrate reabsorption is decreased, whereas it is increased in metabolic acidosis and chronic K^+ depletion, the conditions associated with intracellular acidosis in the proximal tubular cells. Reduction of intracellular pH results in decreased citrate levels in the cytoplasm by increasing citrate entry into the mitochondria via proton-coupled tricarboxylate transport, followed by oxidative phosphorylation (6), and possibly by increasing cytosolic citrate utilization through ATP citrate lyase (47). This change stimulates citrate uptake into the cells, and citrate clearance decreases. Although it has been inferred that the key determinant of hypocitraturia is intracellular acidosis and changes in citrate metabolism, the significance of extracellular (luminal) pH in the alteration of citrate reabsorption was also emphasized (38). Our studies clearly confirm the concept that the pH sensitivity of citrate transport mediated by SDCT1 is due to changes in the proportion between the transported form (Cit^{-2}) and the inhibitory form (Cit^{-3}).

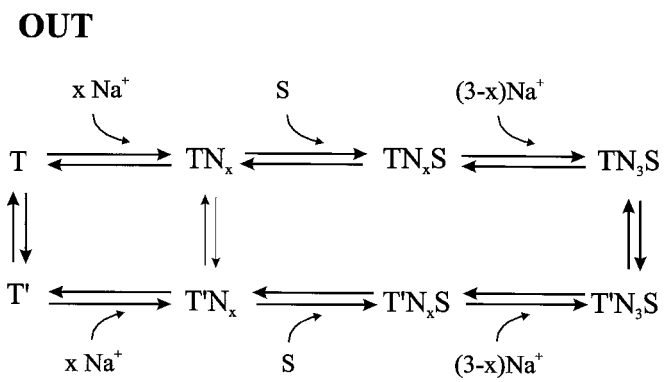

FIG. 10. **Symmetrical ordered kinetic model for SDCT1.** *T* and *T′* indicate the free transporter facing the extracellular and intracellular environments, respectively. *N* = Na^+ and S = substrate. × (= 1 or 2) denotes the number of sodium ions that bind prior to substrate binding. The transition between the conformation states T (TN_3S) and T′ ($T'N_3S$) describes the free (loaded) carrier translocation across the membrane. The sodium leak pathway is described by the transition between states TN_x and $T'N_x$.

There is evidence that apical citrate uptake is regulated by chronic adaptations. Brush border membrane vesicles from chronically K^+-depleted rats demonstrate increases in the maximal rate of the Na^+-coupled citrate transport without changes in the affinities for sodium or citrate (48). Chronic metabolic acidosis in rats also resulted in enhanced citrate transport in brush border membrane vesicles when compared with control rats (23). Future experiments will be needed to determine the regulation of SDCT1 in chronic adaptations.

REFERENCES

1. Wright, S. H., Kippen, I., and Wright, E. M. (1982) *Biochim. Biophys. Acta* **684,** 287–290
2. Wright, S. H., Kippen, I., and Wright, E. M. (1982) *J. Biol. Chem.* **257,** 1773–1778
3. Wright, E. M., Wright, S. H., Hirayama, B., and Kippen, I. (1982) *Proc. Natl. Acad. Sci.* U. S. A. **79,** 7514–7517
4. Wright, S. H., Hirayama, B., Kaunitz, J. D., Kippen, I., and Wright, E. M. (1983) *J. Biol. Chem.* **258,** 5456–5462
5. Wright, E. M. (1985) *Annu. Rev. Physiol.* **47,** 127–141
6. Simpson, D. P. (1983) *Am. J. Physiol.* **244,** F223–F234
7. Ullrich, K. J., Fasold, H., Rumrich, G., and Kloss, S. (1984) *Pflügers Arch. Eur. J. Physiol.* **400,** 241–249

8. Hirayama, B., and Wright, E. M. (1986) *Pfluegers. Arch.* **407,** (Suppl.) 174–179
9. Law, D., Hering-Smith, K. S., and Hamm, L. L. (1992) *Am. J. Physiol.* **263,** C220–C225
10. Brennan, T. S., Klahr, S., and Hamm, L. L. (1986) *Am. J. Physiol.* **251,** F683–F689
11. Barac-Nieto, M. (1984) *Am. J. Physiol.* **247,** F282–F290
12. Wright, S. H., and Wunz, T. M. (1987) *Am. J. Physiol.* **253,** F432–F439
13. Burckhardt, G. (1984) *Pfluegers Arch.* **401,** 254–261
14. Jorgensen, K. E., Kragh-Hansen, U., Roigaard-Petersen, H., and Sheikh, M. I. (1983) *Am. J. Physiol.* **244,** F686–F695
15. Wright, S. H., Kippen, I., Klinenberg, J. R., and Wright, E. M. (1980) *J. Membr. Biol.* **57,** 73–82
16. Fukuhara, Y., and Turner, R. J. (1983) *Am. J. Physiol.* **245,** F374–F381
17. Schell, R. E., and Wright, E. M. (1985) *J. Physiol.* **360,** 95–104
18. Nieth, H., and Schollmeyer, P. (1966) *Nature* **209,** 1244–1245
19. Baruch, S. B., Burich, R. L., Eun, C. K., and King, V. F. (1975) *Med. Clin. N. Am.* **59,** 569–582
20. Pak, C. Y. C. (1987) *Miner. Electrolyte. Metab.* **13,** 257–266
21. Nicar, M. J., Skurla, C., Sakhaee, K., and Pak, C. Y. (1983) *Urology* **21,** 8–14
22. Adler, S., Zett, B., and Anderson, B. (1972) *J. Lab. Clin. Med.* **79,** 505–515
23. Jenkins, A. D., Dousa, T. P., and Smith, L. H. (1985) *Am. J. Physiol.* **249,** F590–F595
24. Asplin, J. R., Favus, M. J., and Coe, F. L. (1996) *The Kidney* (Brenner, B. M., ed.) 5th Ed., pp. 1893–1935, W. B. Saunders Company, Philadelphia, Pennsylvania
25. Pajor, A. M. (1995) *J. Biol. Chem.* **270,** 5779–5785
26. Pajor, A. M. (1996) *Am. J. Physiol.* **270,** F642–F648
27. Khatri, I. A., Kovacs, S. V., Forstner, J. F. (1996) *Biochim. Biophys. Acta* **1309,** 58–62
28. Sekine, T., Watanabe, N., Hosoyamada, M., Kanai, Y., and Endou, H. (1997) *J. Biol. Chem.* **272,** 18526–18529
29. Pajor, A. M., and Sun, N. (1996) *Am. J. Physiol.* **271,** F1093–F1099
30. Pajor, A. M., and Sun, N. (1996) *Am. J. Physiol.* **271,** C1808–C1816
31. Chen, X.-Z., Coady, M. J., and Lapointe, J.-Y. (1996) *Biophys. J.* **71,** 2544–2552
32. Schaeren-Wiemers, N., and Gerfin-Moser, A. (1993) *Histochemistry* **100,** 431–440
33. Chen, X.-Z., Coady, M. J., Jackson, F., Berteloot, A., and Lapointe, J.-Y. (1995) *Biophys. J.* **69,** 2405–2414
34. Segel, I. H. (1975) *Enzyme Kinetics*, pp. 100–143 and 227–242, John Wiley & Sons, New York
35. Umbach, J. A., Coady, M. J., and Wright, E. M. (1990) *Biophys. J.* **57,** 1217–1224
36. Parent, L., Supplisson, S., Loo, D. D., and Wright, E. M. (1992) *J. Membr. Biol.* **125,** 49–62
37. Chen, X.-Z., Coady, M. J., Jalal, F., Wallendorff, B., and Lapointe, J.-Y. (1997) *Biophys. J.* **73,** 2503–2510
38. Hamm, L. L. (1990) *Kidney Int.* **38,** 728–735
39. Hinton, B. T. (1990) *J. Androl.* **11,** 498–505
40. Keil, M., Wetterauer, U., and Heite, H.-J. (1979) *Andrologia* **11,** 385–391
41. Hinton, B. T., and Palladino, M. A. (1995) *Microsc. Res. Tech.* **30,** 67–81
42. Hirayama, B. A., Loo, D. D., and Wright, E. M. (1997) *J. Biol. Chem.* **272,** 2110–2115
43. Castagna, M., Shayakul, C., Trotti, D., Sacchi, V. F., Harvey, W. R., and Hediger, M. A. (1998) *Proc. Natl. Acad. Sci.* U. S. A. **95,** 5395–5400
44. Zerangue, N., and Kavanaugh, M. P. (1996) *Nature* **383,** 634–637
45. Anaizi, N. H., Cohen, J. J., Black, A. J., and Wertheim, S. J. (1986) *Am. J. Physiol.* **251,** F547–F561
46. King, E. L., and Altman, C. (1956) *J. Phys. Chem.* **60,** 1375–1378
47. Melnick, J. Z., Srere, P. A., Elshourbagy, N. A., Moe, O. W., Preisig, P. A., and Alpern, R. J. (1996) *J. Clin. Invest.* **98,** 2381–2387
48. Levi, M., McDonald, L. A., Preisig, P. A., and Alpern, R. J. (1991) *Am. J. Physiol.* **261,** F767–F773